Toxicology and Applied Pharmacology 264 (2012) 65–72

Contents lists available at SciVerse ScienceDirect

Toxicology and Applied Pharmacology

journal homepage: www.elsevier.com/locate/ytaap

Novel bis-(−)-nor-meptazinol derivatives act as dual binding site AChE inhibitors with metal-complexing property

Wei Zheng [a,c,1], Juan Li [b,1], Zhuibai Qiu [a], Zheng Xia [b], Wei Li [a], Lining Yu [c], Hailin Chen [c], Jianxing Chen [c], Yan Chen [b], Zhuqin Hu [b], Wei Zhou [b], Biyun Shao [b], Yongyao Cui [b], Qiong Xie [a,*], Hongzhuan Chen [b,**]

[a] Department of Medicinal Chemistry, School of Pharmacy, Fudan University, 826 Zhangheng Road, Shanghai 200032, PR China
[b] Department of Pharmacology, Institute of Medical Sciences, Shanghai Jiaotong University School of Medicine, 280 South Chongqing Road, Shanghai 200025, PR China
[c] NPFPC Key Laboratory of Contraceptives and Devices, Shanghai Institute of Planned Parenthood Research, 2140 Xietu Road, Shanghai 200032, PR China

ARTICLE INFO

Article history:
Received 30 May 2012
Revised 11 July 2012
Accepted 17 July 2012
Available online 25 July 2012

Keywords:
Bis-(−)-nor-meptazinol derivatives
Acetylcholinesterase inhibitor
Aβ aggregation
Metal chelation

ABSTRACT

The strategy of dual binding site acetylcholinesterase (AChE) inhibition along with metal chelation may represent a promising direction for multi-targeted interventions in the pathophysiological processes of Alzheimer's disease (AD). In the present study, two derivatives (ZLA and ZLB) of a potent dual binding site AChE inhibitor bis-(−)-nor-meptazinol (bis-MEP) were designed and synthesized by introducing metal chelating pharmacophores into the middle chain of bis-MEP. They could inhibit human AChE activity with IC_{50} values of 9.63 μM (for ZLA) and 8.64 μM (for ZLB), and prevent AChE-induced amyloid-β (Aβ) aggregation with IC_{50} values of 49.1 μM (for ZLA) and 55.3 μM (for ZLB). In parallel, molecular docking analysis showed that they are capable of interacting with both the catalytic and peripheral anionic sites of AChE. Furthermore, they exhibited abilities to complex metal ions such as Cu(II) and Zn(II), and inhibit Aβ aggregation triggered by these metals. Collectively, these results suggest that ZLA and ZLB may act as dual binding site AChEIs with metal-chelating potency, and may be potential leads of value for further study on disease-modifying treatment of AD.

Introduction

Alzheimer's disease (AD) is a progressive neurodegenerative disorder, with extracellular senile plaques formed by aggregates of amyloid-β (Aβ) as one of the most prominent neuropathological hallmarks, which may trigger cholinergic dysfunction in brain (Mancuso et al., 2010; Schliebs and Arendt, 2011). To date, acetylcholinesterase inhibitors (AChEIs), such as tacrine, donepezil, galantamine and rivastigmine, are the main approved agents for AD therapy. However, they do not retard the neurodegenerative processes, although beneficial in improving cognitive and behavioral symptoms. The multifactorial nature of AD strongly suggests that combination therapy with several drugs intervening in various pathophysiological processes or compounds capable of interacting with several molecule targets involved in the neurotoxic cascade may have disease-modifying effects. While multiple-medication therapy may have potential disadvantages to AD patients such as ADME interactions and poor compliance, one-compound-multiple-target strategy may be more favorable in AD treatment. In recent years, several multifunctional agents capable of hitting different biological targets have been developed, and their biological profiles seem to be promising (Bajda et al., 2011; Fernández-Bachiller et al., 2010; Minarini et al., 2012).

Biochemical and neuropathological evidence converge to suggest that dyshomeostasis of cerebral biometals (such as copper, zinc and iron) plays crucial roles in Aβ aggregation and neurotoxicity, which are central in neurodegeneration related to AD (Duce and Bush, 2010; Hung et al, 2010). In amyloid plaques, elevated concentrations of Cu(II) and Zn(II) have been detected by spectroscopic studies, and in in vitro experiments these metals are able to bind to Aβ and promote its aggregation. Furthermore, redox-active metal ions like copper and iron contribute to production of reactive oxygen species (ROS) and oxidative stress, which are early events of neurodegeneration. Therefore, metal chelation may represent a rational therapeutic approach for interdicting AD pathogenesis. Several lipophilic metal chelators such as clioquinol and its derivative PBT2 have been studied in clinical trials and shown encouraging results in some AD patients (Faux et al., 2010; Guay, 2004).

The recent discovery of the so-called "nonclassical function" of AChE has renewed interest in search for novel AChEIs with real disease-modifying potency. It has been reported that AChE might

Abbreviations: AD, Alzheimer's disease; Aβ, amyloid-β; AChE, acetylcholinesterase; AChEIs, acetylcholinesterase inhibitors; ADME, absorption, distribution, metabolism and excretion; ROS, reactive oxygen species; ACh, acetylcholine; MEP, meptazinol; LAH, lithium aluminum hydride; THF, tetrahydrofuran; HFIP, 1,1,1,3,3,3-hexafluoro-2-propanol; DTPA, diethylenetriaminepentaacetic acid; CCK-8, cell counting kit-8; TcAChE, *Torpedo californica* AChE.

* Corresponding author. Fax: +86 21 51980122.
** Corresponding author. Fax: + 86 21 64674721.
E-mail addresses: yaoli@shsmu.edu.cn (H. Chen), xiejoanxq@gmail.com (Q. Xie).
[1] These authors contributed equally to this work.

0041-008X/$ – see front matter © 2012 Elsevier Inc. All rights reserved.
http://dx.doi.org/10.1016/j.taap.2012.07.018

act as a pathological chaperone in inducing Aβ fibrillogenesis through direct interactions of its peripheral anionic site with the peptide (Inestrosa et al., 2008; Johnson and Moore, 2006). In light of this, AChEIs that simultaneously block both the catalytic and peripheral sites might not only alleviate the cognitive deficit of AD patients by elevating acetylcholine (ACh) levels, but also act as disease-modifying agents via delaying amyloid plaque formation.

In our previous study based on (−)-meptazinol (MEP), a compound exhibiting moderate potency of AChE inhibition (Ennis et al., 1986), we developed a homo-bivalent (−)-MEP derivative, bis-(−)-nor-MEP (bis-MEP), as an effective drug candidate for AD therapy (Xie et al., 2008). This compound has multiple functions, e.g., inhibiting AChE activity and preventing AChE-induced Aβ aggregation, with an acceptable safety profile (LD_{50} = 313 mg/kg). Computational analysis and subsequent crystallographic studies have demonstrated that bis-MEP is able to simultaneously interact with both catalytic and peripheral anionic sites of the enzyme (Paz et al., 2009; Xie et al., 2008).

Recently, in a search for new rationally-designed multifunctional agents against AD, we started from the dual binding site AChEI bis-MEP, and focused on the spacer as the carrier of a third biological activity. As the important role of transition metal ions in Aβ aggregation, metal chelation pharmacophores were introduced into the middle chain of bis-MEP, with an intention to endow additional metal-complexing potency while keeping its other multifunctional profiles. A successful modification has been obtained by incorporating oxalamide functionality as a chelation pharmacophore into the spacer of bis-tacrine (Bolognesi et al., 2007). Ethylenediamine is a bidentate ligand which can form stable complexes with various metal ions, such as Cu(II)–ethylenediamine complex (Inada et al, 1993). Therefore, we rationally designed two novel bis-MEP derivatives N^1,N^2-bis(3-((S)-3-ethyl-3-(3-hydroxyphenyl)azepan-1-yl)propyl)oxalamide hydrochloride (ZLA) and N^1,N^2-bis(3-((S)-3-ethyl-3-(3-hydroxyphenyl) azepan-1-yl)propyl)-ethane-1,2-diamine hydrochloride (ZLB) with promising profiles of dual binding site AChE inhibition and metal chelation (Fig. 1). Their properties of dual binding site AChE inhibition and Cu(II) or Zn(II) chelation were evaluated in the present study.

Material and methods

Preparation of N^1,N^2-bis(3-chloropropyl) oxalamide (oxalamide). Oxalyl dichloride (1.27 g, 10.0 mmol) in $CHCl_3$ (10 mL) was added to a solution of 3-chloropropylamine hydrochloride (2.6 g, 20.0 mmol), NaOH (2 g) and H_2O (4 mL) in $CHCl_3$ (20 mL) at 0 °C. The mixture was stirred at 0 °C for 20 min, extracted with $CHCl_3$ (20 mL×3) and dried with anhydrous $MgSO_4$. Evaporation of the solvent gave oxalamide (2.40 g, 99.6%) a yellowish powder. Recrystallization of crude oxalamide from ethyl acetate afforded oxalamide as white needle-like crystals (1.61 g, 67.1%). Melting points (mp) 169–170 °C. ^{1}H NMR ($CDCl_3$): Chemical shifts (δ) 7.65 (s, 2H, NHCO), 3.59 (t, 4H, J = 6 Hz, Cl−CH_2), 3.51 (dd, 4H, J_1 = 7 Hz, J_2 = 13 Hz, N−CH_2), 2.08–2.02 (m, 4H, CH_2); MS (ESI): 241.0 $[M+H]^+$; 263.0 $[M+Na]^+$.

Synthesis of ZLA. Detailed synthetic procedure for the intermediates (−)-normethyl-MEP (nom-MEP) was described in our previous studies (Xie et al., 2008). Triethylamine (0.8 mL, 5.75 mmol) and oxalamide (0.35 g, 1.45 mmol) were added to a solution of nom-MEP (0.79 g, 3.60 mmol) in acetonitrile. The reaction mixture was refluxed for 20 h and evaporated. The residue was diluted with saturated Na_2CO_3 solution (10 mL), extracted with $CHCl_3$ and then dried with anhydrous Na_2SO_4 and evaporated. The residue was purified by column chromatography on silica gel using $CHCl_3$/CH_3OH (93:7) as eluent. Addition of dry HCl–ether to a solution of the above purified compound (0.53 g, 60.2%) in dry ether and adjusting pH to 3–4 gave the hydrochloride salt ZLA (0.37 g, 62.3%) as white powder. mp. 154–157 °C, specific rotation ($[\alpha]_D^{20}$) = −7.7° (c = 0.390, MeOH). ^{1}H NMR (DMSO-d_6): δ10.30 and 10.14 (br s, 4/3 H, NH^+), 9.59, 9.50 (s, 2H, ArOH), 8.98–8.96 (m, 2H, NHCO), 8.63 and 8.55 (br s, 2/3 H, NH^+), 7.27–7.20 (m, 2H, ArH), 6.91–6.75 (m, 6H, ArH), 3.89 (d, 2/3 H, J = 13.6 Hz, N−CH_2), 3.57 (d, 4/3 H, J = 14.1 Hz, N−CH_2), 3.42 (m, 2H, N−CH_2), 3.32–3.18 (m, 12H, N−CH_2), 2.46–2.41 (m, 1H, CH_2), 2.25–2.13 (m, 5H, CH_2), 2.08–2.01 (m, 2H, CH_2), 1.98–1.79 (m, 9H, CH_2), 1.61–1.48 (m, 3H, CH_2), 0.57 (t, 6H, J = 7.3 Hz, CH_3); MS (ESI): 607.5 $[M+H]^+$, 304.3 $[M+2H]^{2+}$; ^{13}C NMR (DMSO-d_6): δ 160.08, 160.01, 157.55, 157.47, 144.82, 143.64, 129.42, 129.25, 117.23, 116.89, 114.10, 113.57, 113.49, 113.30, 63.68, 61.35, 58.63, 57.13, 56.58,

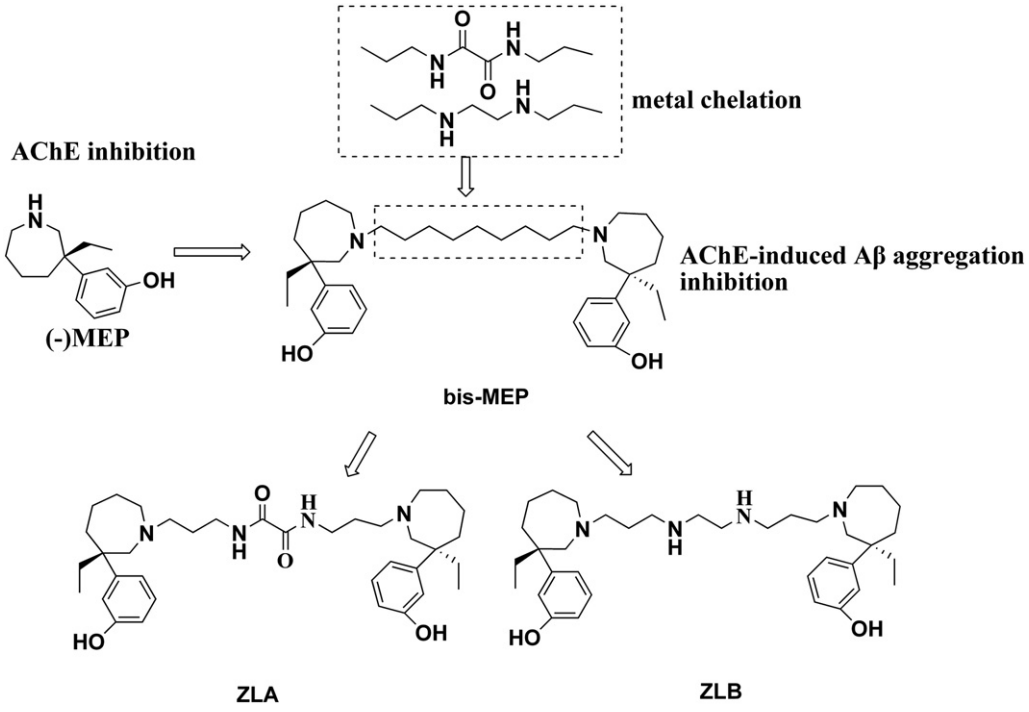

Fig. 1. Design strategy for new multifunctional compounds.

56.31, 43.70, 43.37, 36.39, 36.20, 35.33, 35.26, 34.43, 33.05, 26.33, 24.88, 22.84, 22.79, 20.76, 20.46, 8.10, 7.96; MS (ESI): 607.5 $[M+H]^+$, 304.3 $[M+2H]^{2+}$.

Synthesis of ZLB. A solution of ZLA (0.53 g, 0.87 mmol) in dry tetrahydrofuran (THF, 20 mL) was added to lithium aluminum hydride (0.23 g, 6.05 mmol) in dry THF (10 mL) at room temperature. The mixture was refluxed for 24 h, and then H_2O (0.23 mL), 15% NaOH (0.23 mL) and H_2O (0.69 mL) were added. The mixture was stirred for 15 min at room temperature and filtered; the solid material was washed with THF and evaporated. The residue was treated with H_2O (15 mL), and aqueous ammonia was added to adjust the pH to 9. The mixture was extracted with $CHCl_3$, dried with anhydrous Na_2SO_4 and concentrated in vacuo to give a residue (0.51 g) as a yellow oil, which was purified using silica gel column chromatography with $CHCl_3/CH_3OH$ (95:5) as eluent, and then converted to final salt in dry HCl–ether solution to afford ZLB as white powder (115 mg, 18.1%). mp. 132–136 °C, $[\alpha]_D^{20} = -27.1°$ (c = 0.240, MeOH). ^{1}H NMR (DMSO-d_6): δ10.26 and 10.19 and 9.94 and 9.83 (br s, 4H, NH^+), 9.51, 9.43 (s, 2H, ArOH), 8.77 and 8.26 and 8.17 (s, 2H, NH), 7.22–7.13 (m, 2H, ArH), 6.90–6.69 (m, 6H, ArH), 3.94 (m, 2/3 H, N–CH_2), 3.57 (m, 4/3 H, N–CH_2), 3.32–2.80 (m, 14H, N–CH_2), 2.41–2.01 (m, 8H, CH_2), 1.98–1.67 (m, 9H, CH_2), 1.53–1.47 (m, 3H, CH_2), 0.51 (t, 6H, J = 7.4 Hz, CH_3); MS (ESI): 579.4 $[M+H]^+$, 290.4 $[M+2H]^{2+}$; ^{13}C NMR (DMSO-d_6): δ157.55, 157.45, 144.77 and 144.70, 143.84, 129.56, 129.29, 117.34, 117.03, 113.94, 113.60, 113.50, 113.31, 63.99 and 63.85, 61.33, 58.59, 56.23, 55.97, 55.88, 43.98, 43.82, 43.43, 40.00, 36.16, 35.39, 35.09, 35.07, 33.14, 32.98, 26.38 and 26.34, 25.18, 21.22, 20.72 and 20.31, 19.93 and 19.49, 18.50, 10.91, 8.12 and 8.01; MS (ESI): 579.4 $[M+H]^+$, 290.4 $[M+2H]^{2+}$.

Molecular docking. To confirm that substitution of the aliphatic spacer of bis-MEP with metal chelation pharmacophores does not negatively affect the ability for the new compounds to interact with AChE, molecular docking simulations were performed on an R14000 SGI Fuel workstation with the software package SYBYL 6.9 (Tripos, St. Louis, MO, USA). Standard parameters were used unless otherwise indicated. The crystal structure of *Torpedo californica* AChE (TcAChE) was obtained from the Protein Data Bank (PDB code 1EA5). Heteroatoms and water molecules in the proteins were removed, and hydrogen atoms were subsequently added. Bis-MEP derivatives were drawn in ISIS/Base with ISIS/Draw from MDL and exported into a 2D structure data file (SDF) to form a small focused library. The 2D structures of the library were subsequently converted into 3D structures with CORINA, still in SDF format. The 3D structures were then read into SYBYL Molecular SpreadSheet table for further treatment, such as energy minimization for 100 steps with Tripos force field and Gasteiger–Marsili charges for each molecule. These structures were put into databases and then written to MOL2 files as input. Molecular docking was carried out using GOLD 3.0 (CCDC, Cambridge, UK, 2005) to generate an ensemble of docked conformations for the ligand. The active site was defined as all atoms within a radius of 25 Å around Tyr121*O*_ of *Tc*AChE. This enlarged binding pocket was chosen, as a smaller one might neither accommodate a large bis-ligand nor include both the catalytic and peripheral sites of AChE. Because of the high flexibility of the ligand, which contains many rotatable bonds, 600 genetic algorithm (GA) runs were performed rather than the default of 10. For each GA run, the default GA settings were used, except that early termination was prohibited and pyramidal nitrogen inversion was allowed.

Log P determination. Partition coefficients of ZLA and ZLB were determined by shake-flask method in the octanol/phosphate buffer solution at pH 4, 5, 6, 7, 7.4 or 8. The phosphate buffer and octanol were saturated with each other prior to partitioning by mixing and allowing the phases to separate overnight. A stock solution for each compound was prepared at 0.1 mg/mL in phosphate buffer-saturated octanol. Then 1.0 mL sample solution and 1.0 mL octanol-saturated phosphate buffer were pipetted into a centrifuging tube and shaken for 48 h at 37 °C, followed by centrifuging for 5 min (2000 rpm), the aqueous phase was separated and analyzed with reversed phase-high performance liquid chromatography (RP-HPLC). The mobile phase was methanol/0.02 mol/L ammonium acetate solution (75:25; pH was adjusted to 7.4 with aqueous ammonia) at a flow rate of 1.0 mL/min through a VP-ODS column (250 mm × 4.6 mm, 5 μm; Shimadzu, Kyoto, Japan) at 50 °C. Experiments were conducted in triplicate and log P values were calculated.

In vitro cholinesterase inhibition assay. Inhibitory potency against mice or human-derived AChE of ZLA or ZLB was evaluated by a modified Ellman's method (Bartolini et al., 2003; Li et al., 2007). Mice forebrain homogenates, which were prepared in normal saline (1:9 w/v) and used as a source of AChE, were pre-incubated with the tested inhibitors at various concentrations for 20 min at 37 °C in 0.05 M phosphate buffered solution (pH 7.2), containing 250 μM 5,5′-dithio-bis(2-nitrobenzoic) acid (DTNB). Then acetylthiocholine iodide (500 μM) was added as the substrate, and AChE activity was determined by UV spectrophotometry at 412 nm. The concentration of compounds that produced 50% inhibition of the AChE activity (IC_{50}) was calculated by nonlinear regression of the response–concentration (log) curve. As for determination of inhibition of human AChE activity, AChE stock solution was prepared by dissolving human recombinant AChE lyophilized powder (Sigma, St. Louis, MO, USA) in 0.1 M phosphate buffer (pH 8.0) containing 0.1% Triton X-100. The assay solution consisted of a 0.1 M phosphate buffer pH 8.0, with the addition of 340 μM DTNB, 0.5 unit/mL human recombinant AChE and 550 μM substrate (acetylthiocholine iodide). Butyrylcholinesterase (BChE; derived from mice sera, 1:19 w/v in normal saline) inhibition was similarly carried out using butyrylthiocholine iodide (500 μM) as the substrate. Results are reported as the mean ± SEM of IC_{50} obtained from at least three independent measures.

Inhibition of AChE-induced Aß aggregation. According to descriptions of the previous studies (Bartolini et al., 2003), aliquots of 2 μL Aβ1–40 peptide (Invitrogen, Carlsbad, CA. USA), lyophilized from 1 mg/mL 1,1,1,3,3,3-hexafluoro-2-propanol (HFIP; Sigma) solution (HFIP was used as a solvent to ensure that AChE-induced Aβ aggregation started with an Aβ solution mainly random coil or α-helix structure, which is poorly amyloidogenic) and dissolved in dimethyl sulfoxide (DMSO), were incubated for 48 h at room temperature in 0.215 M sodium phosphate buffer (pH 8.0) at a final concentration of 230 μM. For co-incubation experiments, aliquots (16 μL) of human recombinant AChE (with the molar ratio of Aβ/AChE as 100:1; Sigma) and AChE in the presence of 2 μL of the tested inhibitors at various concentrations were added. The final volume of each vial was 20 μL. Each assay was run in duplicate.

To quantify amyloid fibril formation, the thioflavin T fluorescence method was then applied. After incubation, the samples containing Aβ, Aβ plus AChE, or Aβ plus AChE in the presence of the test inhibitors were diluted with 50 mM glycine–NaOH buffer (pH 8.5) containing 1.5 μM thioflavin T (Sigma) to a final volume of 2.0 mL. Fluorescence was monitored by PE LS45 spectrophotometer (Perkin Elmer, Waltham, MA, USA), with excitation at 446 nm and emission at 490 nm. A time scan of fluorescence was performed, and the intensity values reached at the plateau (around 300 s) were averaged after subtracting the background fluorescence from 1.5 μM thioflavin T and AChE. The percent inhibition of the AChE-induced aggregation due to the presence of increasing concentrations of test compounds was calculated by the following formula: $100 - (IFi/IFo \times 100)$, where IFi and IFo were the fluorescence intensities obtained for Aβ plus AChE in the presence and in the absence of the inhibitors, respectively, after subtracting the fluorescence of respective blanks. Inhibition curves and linear regression parameters were obtained for each compound, and the IC_{50} was extrapolated.

Metal-chelating properties. The ability for compounds ZLA, ZLB or bis-MEP to chelate biometals such as Cu(II) was studied by UV–vis spectrometry (Baum and Ng, 2004). The absorption spectra of ZLA, ZLB or bis-MEP, alone (in methanol) or in the presence of $CuCl_2$ (with a molar ratio of 1:1), were recorded at a duration of 30 min at room temperature in a 1 cm quartz cell using Multiscan MK3 spectrophotometer (Thermo, Waltham, MA, USA). Additionally, the ratio of ligand/metal ion in the complex was determined by molar ratio method (Bolognesi et al., 2007). Fixed concentrations of the compounds (25 μM) was mixed with ascending doses of $CuCl_2$ (12–40 μM) and the UV–vis absorption spectra were recorded.

Aggregation assay by sedimentation. Aβ1–40, lyophilized from 1 mg/mL HFIP solution, was dissolved in DMSO to get a 500 μM stock solution, and was brought to 10 μM in 20 mM Hepes buffer, 150 mM NaCl alone or with metal ions (20 μM), in the presence or absence of the tested compounds (100 μM). The reaction mixture (100 μL) was incubated for 15 min at 37 °C, and then centrifuged at 13,000×g for 15 min to sediment aggregated proteins. Peptide concentration in the supernatant was determined by the Bradford method using the commercial protein assay Coomassie Brilliant Blue solution (Thermo) and was represented as a percentage of recovery relative to the control without metal ions and tested compounds (Atwood et al., 1998; Raman et al., 2005). As AD is complicated by cerebral acidosis with a pH of 6.6 (Yates et al., 1990), 20 mM Hepes buffer, 150 mM NaCl was set to pH 6.6 with hydrochloric acid in this assay.

Turbidometric assay. Turbidity measurements, also as an assay for aggregation, were performed according to the method described in the previous studies (Atwood et al., 1998). The stock solution of Aβ1–40 (500 μM) was brought to 10 μM in 20 mM Hepes buffer, 150 mM NaCl (pH 6.6) alone or with metal ions (20 μM), in the presence or absence of the tested compounds (100 μM). The reaction mixture (200 μL) was incubated for 30 min at 37 °C, and absorbance (405 nm) was measured using a Varioskan Flash spectrophotometric microplate reader (Thermo). Automatic 30-s plate agitation mode was selected for the plate reader to evenly suspend the aggregates in the wells before all readings.

Determination of cell viability. The human neuroblastoma cell line SH-SY5Y cells (American Type Culture Collection, Manassas, VA, USA) were cultured in MEM/F-12 (1:1) medium (Invitrogen) supplemented with 10% fetal calf serum (FCS; Invitrogen), 100 U/mL penicillin, and 100 μg/mL streptomycin in a humidified atmosphere containing 5% CO_2 at 37 °C. Cells were plated at 5×10^4 cells/well (100 μL) into 96-well plates and allowed to adhere and grow. When cells reached the required confluence, they were placed into serum-free medium and treated with ZLA or ZLB. Twenty-four hours later the survival of cells was determined by Cell Counting Kit-8 (CCK-8; Dojindo, Japan) assay. Briefly, after incubation with 10 μL of CCK-8 (5 mg/mL) at 37 °C for 2 h, the absorbance was measured with a test wavelength of 570 nm and a reference wavelength of 655 nm. The absorbance of control cells was set to 100%, and the percentage of viable cells collected from each treatment was calculated relative to the control group.

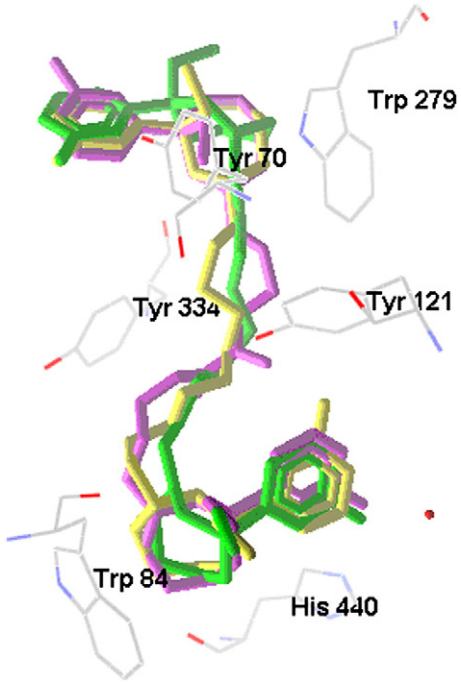

Fig. 2. Binding modes of bis-MEP, ZLA and ZLB (green, purple and yellow, respectively) at the *Tc*AChE gorge. ZLA and ZLB are able to properly contact with both sites of the enzyme. The two MEP moieties establish π–π stacking with Trp84, Trp279 and Tyr70, while the spacer does not seem to be detrimental to the interactions with the enzyme. Worthy to note, some interactions could be identified for ZLA and ZLB with Tyr121, although they are not strong enough to increase the AChE inhibitory potency.

Data analysis and statistics. Values are expressed as mean ± SEM. Comparisons among means were performed using one-way ANOVA and post hoc by Dunnett test. Differences with *P* values less than 0.05 were considered statistically significant.

Results

Molecular docking studies of ZLA and ZLB

The results of molecular docking demonstrate that compounds ZLA and ZLB are able to interact with both the catalytic and peripheral anionic sites of AChE (Fig. 2). It is worth noting that replacement of the nonylene spacer with oxalamide or ethylenediamine may reduce AChE binding affinity as compared with their prototype bis-MEP. And, although the derivatives could establish favorable interactions with some mid-gorge residues, the increased polarity of ZLA and ZLB may result in a major energy penalty during their desolvation.

Log P of ZLA and ZLB

The partition coefficients of ZLA and ZLB in the octanol/phosphate buffer solution at different pH (4, 5, 6, 7, 7.4 and 8 respectively) were determined by the classical shake-flask method using RP-HPLC. As

Table 1
pH-dependent partition coefficients (log P) of ZLA and ZLB.

Compounds	Log P					
	pH 4	pH 5	pH 6	pH 7	pH 7.4	pH 8
ZLA	0.18 ± 0.001	0.22 ± 0.002	1.11 ± 0.001	2.69 ± 0.003	3.71 ± 0.003	4.06 ± 0.006
ZLB	0.38 ± 0.001	0.39 ± 0.001	1.78 ± 0.003	3.07 ± 0.005	4.00 ± 0.004	4.22 ± 0.003

The partition coefficients of ZLA and ZLB in the octanol/buffer solution at different pH (4, 5, 6, 7, 7.4 and 8 respectively) were determined by the classical shake-flask method. The data represent the mean ± SEM of three independent experiments.

Table 2
Inhibition of ZLA and ZLB on AChE or BChE activity.

Compounds	$IC_{50} \pm SEM$ (μM)			Selectivity for mice AChE
	Human recombinant AChE	Mice AChE	Mice BChE	
ZLA	9.63 ± 1.64	1.81 ± 0.36	1.33 ± 0.26	0.73
ZLB	8.64 ± 1.58	1.54 ± 0.27	1.72 ± 0.30	1.12
Rivastigmine	8.45 ± 1.47	5.43 ± 0.83	2.13 ± 0.47	0.39

AChE, acetylcholinesterase. BChE, butyrylcholinesterase. Mice forebrain homogenates prepared in normal saline were used as a source of AChE. Mice sera were the source of BChE. AChE or BChE activity was assayed spectrophotometrically at 412 nm. IC_{50} values represent the concentration of inhibitors required to decrease enzyme activity by 50% and are the mean ± SEM of three independent measurements.

Table 3
Inhibition of ZLA and ZLB on human AChE-induced Aβ aggregation.

Compounds	$IC_{50} \pm SEM$ (μM)	Inhibition (%) at 100 μM	Inhibition (%) at 200 μM
ZLA	49.1 ± 5.0	53.2 ± 4.3	55.6 ± 4.7
ZLB	55.3 ± 5.8	45.3 ± 4.2	48.4 ± 4.3
Propidium iodide	11.9 ± 0.4	80.2 ± 4.9	94.3 ± 5.3

AChE, acetylcholinesterase. Aβ, amyloid-β. Human recombinant AChE-induced Aβ fibrillogenesis was determined using thioflavin T fluorescence. The final concentration of Aβ1–40 was 230 μM, and the molar ratio of Aβ1–40/AChE was equal to 100/1. The data represent the mean ± SEM of three independent experiments.

Table 1 shows, the lipophilicity of the two compounds increased with the rise of pH values. With log P values of 3.71 and 4.00 respectively at the physiological pH 7.4, ZLA and ZLB are sufficiently lipophilic to pass the blood brain barrier (BBB).

AChE/BChE inhibitory activity of ZLA and ZLB

To determine the potential value of newly synthesized compounds for the treatment of AD, their inhibitory potency for AChE or BChE was assayed, with rivastigmine as a reference compound. As Table 2 shows, ZLA and ZLB exhibited smaller IC_{50} values for mice AChE or BChE inhibition or similar IC_{50} values for human AChE activity inhibition compared with rivastigmine, suggesting that their potency for cholinesterase inhibition is comparable to rivastigmine. The inhibition–concentration curves of ZLA and ZLB on human AChE activity are demonstrated in Fig. 3.

Inhibition of AChE-induced Aβ aggregation by ZLA and ZLB

It has been established that the peripheral anionic site mediates AChE-triggered Aβ aggregation (Inestrosa et al., 2008; Johnson and Moore, 2006). In the present study, the inhibition and IC_{50} values of ZLA or ZLB on human recombinant AChE-induced Aβ fibrillogenesis, in comparison with the selective peripheral site-binding inhibitor propidium iodine, was determined by means of a thioflavin T-based fluorometric assay (Bartolini et al., 2003). As Table 3 shows, both ZLA and ZLB inhibited AChE-promoted Aβ aggregation, with IC_{50} values of 49.1 and 55.3 μM respectively. At the dose of 100 μM, these compounds could inhibit fibrillogenesis by nearly 50%. Similar with the results of the previous studies (Bartolini et al., 2003), propidium iodine, used as a positive reference, exhibited more potent inhibition of AChE-promoted Aβ aggregation (Table 3). The inhibition–concentration curves of ZLA and ZLB on human AChE-triggered fibrillogenesis are shown in Fig. 4.

Metal-chelating properties of ZLA and ZLB

When ZLA or ZLB in methanol solution were mixed with equal molar of $CuCl_2$, a spectral change was observed, which was not dependent on time after mixing and appeared to be attributed to complex formation between the compounds and Cu(II) (Figs. 5A, B). In the case of the Cu(II)–ZLA complex, Cu(II) binding led to a decrease in absorption at 200–208 nm and a bathochromic shift with a maximum peak at 220 nm resulting from charge transfer processes between the coordinated oxalamide and metal. The spectra of Cu(II)–ZLB complex showed an increase in molar absorbance, whereas bis-MEP mixed with $CuCl_2$ produced no significant spectral change (Fig. 5C), indicating that the metal binding is due to specific interactions of the spacer moiety in these bis-MEP derivatives with metal ions. The absorption spectra of mixtures of ZLA with ascending concentrations of $CuCl_2$ (12–40 μM) are shown in Fig. 6. It was observed that the spectra reached to maximal intensity at 1:1 molar ratio, suggesting a 1:1 of stoichiometry of the complex.

Inhibition of metal ion-induced Aβ aggregation by ZLA and ZLB

To further assess the metal-complexing property, we subsequently observed the effects of ZLA or ZLB on Aβ aggregation triggered by Cu(II) or Zn(II) by sedimentation and turbidometry, which gave consistent results (Figs. 7A, B). Similar with the results of previous studies (Atwood et al., 1998; Raman et al., 2005), Cu(II) and Zn(II) induced markedly aggregation of Aβ, manifested as decreased percentage of recovery and increased turbidity. ZLA or ZLB (at a concentration of 100 μM) dramatically suppressed metal ion-induced aggregation of the peptide as measured by both sedimentation and turbidometry ($P<0.01$ versus Cu(II) + Aβ or Zn(II) + Aβ). These findings, in parallel with those of spectroscopic analyses, indicate that ZLA or ZLB may effectively chelate with biometal ions such as Cu(II) or Zn(II), and inhibit metal ion-promoted Aβ aggregation. ZLA and ZLB, at 100 μM, did not exhibit notable effect on the aggregation of Aβ (data not shown).

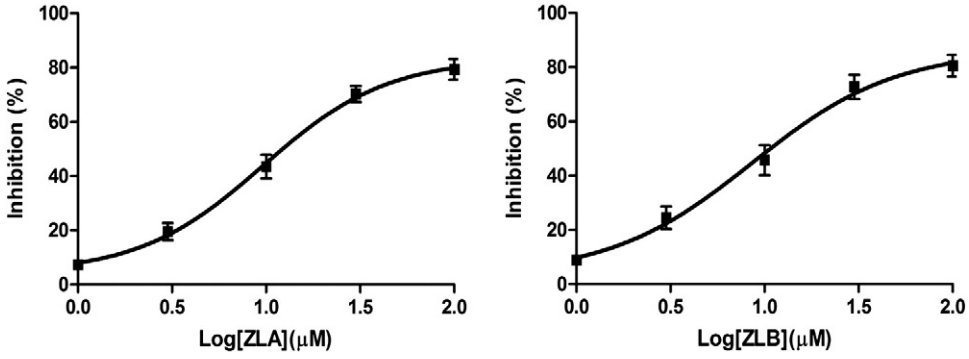

Fig. 3. Inhibition–concentration curves of ZLA and ZLB on human acetylcholinesterase (AChE) activity in vitro. Each point represents the mean ± SEM of three independent experiments.

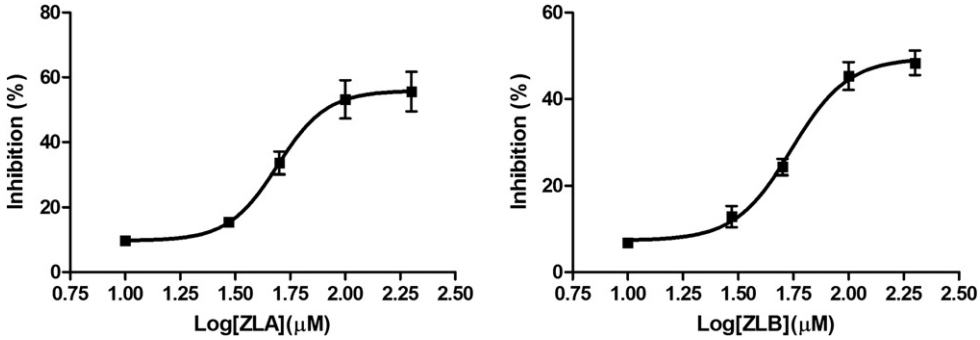

Fig. 4. Inhibition–concentration curves of ZLA and ZLB on human acetylcholinesterase (AChE)-induced amyloid-β (Aβ) fibrillogenesis in vitro. Each point represents the mean ± SEM of three independent experiments.

Cell viability

The cytotoxicity of compounds ZLA or ZLB was determined in human neuroblastoma cell line SH-SY5Y with CCK-8 assay. The survival of cells treated with ZLA or ZLB at concentrations of 1, 10 or 100 μM was not significantly different from that of control group. The percentage cell viability of ZLA (1, 10, 100 μM)-treated cells was 99.2 ± 9.4, 96.8 ± 8.7 and 89.2 ± 8.4 respectively, and that for ZLB-treated cells was 99.8 ± 9.9, 97.3 ± 9.1 and 90.4 ± 8.6 respectively.

Discussion

The multifactorial nature of AD and the potential disadvantages of multiple-medication therapy in clinical practice (such as drug–drug interactions and compliance problems) have prompted the research efforts to discover multifunctional pharmaceuticals. In designing novel multi-target-directed ligands against AD, dual binding site AChEIs have been regarded as a suitable starting point. These ligands show potential of alleviating the cognitive deficit in AD by restoring

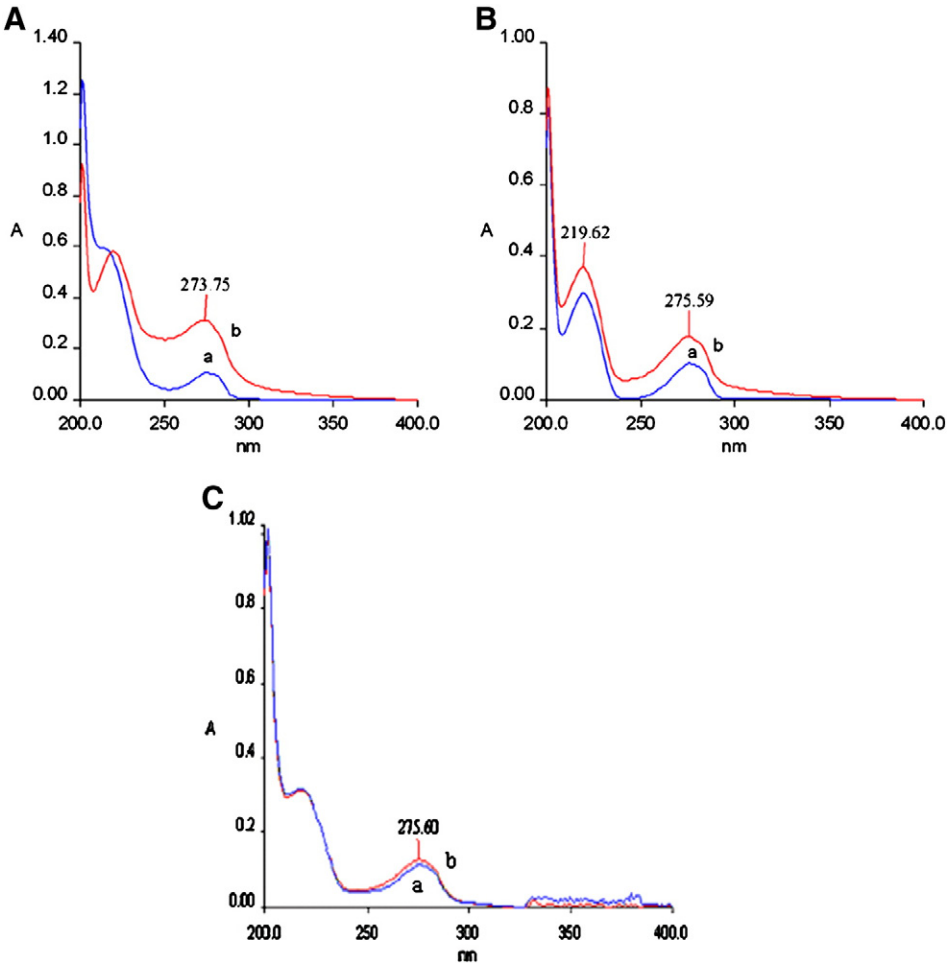

Fig. 5. UV–vis (200–400 nm) absorption spectra of ZLA, ZLB or bis-MEP alone (25 μM in methanol; blue line) or mixed with Cu(II) (25 μM; red line) for 30 min. A) a, ZLA; b, ZLA + $CuCl_2$; B) a, ZLB; b, ZLB + $CuCl_2$; C) a, bis-MEP; b, bis-MEP + $CuCl_2$.

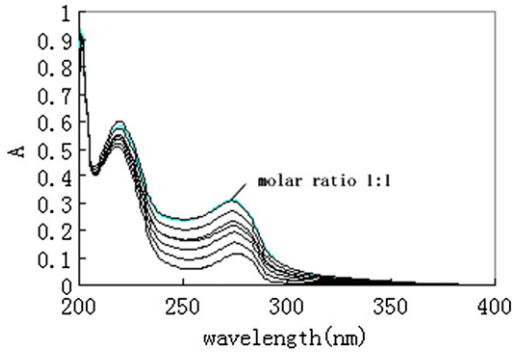

Fig. 6. UV–vis (200–400 nm) absorption spectra of ZLA (25 μM) in methanol after addition of ascending concentrations of $CuCl_2$ (12–40 μM).

cholinergic activity. More importantly, they show disease-modifying potential via inhibiting AChE-induced Aβ aggregation. Increasing evidence demonstrates that rational modification of their molecular structures, with the intention to provide them with additional biological properties, is a promising strategy for development of drugs with multi-target-directed properties for AD treatment (Bajda et al., 2011; Bolognesi et al., 2007).

Based on a 'pharmacophore conjugation' concept, we designed novel compounds ZLA and ZLB based on bis-MEP, a dual binding site AChEI we have reported previously (Xie et al., 2008). The results of functional experiments demonstrate that these compounds exhibit multiple functions, e.g., inhibiting AChE activity (comparable to rivastigmine) and preventing AChE-induced Aβ aggregation with IC_{50} values compatible to those for AChE inhibition. These findings, in line with those of molecular docking, confirm that ZLA and ZLB are effective dual binding site AChEIs, which can simultaneously carry out the anti-cholinesterase and anti-aggregating actions.

It is worth noting that ZLA and ZLB displayed no obvious selectivity for AChE. In recent years, accumulating evidence has indicated that BChE is likely to be involved in the pathology of AD, and inhibition of BChE may ameliorate cognitive dysfunction related to AD (Furukawa-Hibi et al., 2011; Greig et al., 2005). Therefore, agents that inhibit both AChE and BChE may be of more benefit to AD patients (Venneri et al., 2005).

The results of UV–vis absorption spectrometry showed that ZLA and ZLB exhibit Cu(II)-complexing property with stoichiometry of 1:1. Moreover, sedimentation and turbidity assay revealed that they markedly inhibit Cu(II) or Zn(II)-triggered Aβ aggregation. These results suggest that ZLA and ZLB might act against Aβ neurotoxicity by a metal complexing mechanism besides dual binding site AChE inhibition, and thus may be promising in intervention of AD progression by hitting multiple targets involved in AD pathogenesis. It is worth noting that, it is controversial about the role of metals in the pathogenesis of AD. For example, there is evidence suggesting that copper may both promote and prevent AD progression (Quinn et al., 2009). However, it is recently demonstrated that AD is characterized by copper derangement manifested as intracellular deficiency while extracellular excess (Cater et al., 2008), and transgenic AD mice receiving agents with copper-chelating property exhibit attenuated Aβ pathology (Quinn and Harris, 2010).

The results of cell viability assay with SH-SY5Y cell line showed no apparent cell toxicity of ZLA and ZLB at doses of 1–100 μM. More encouragingly, these compounds show favorable partition coefficients under the physiological pH 7.4, suggesting that they are sufficiently lipophilic to pass BBB. This is of special importance for development of new lead compounds for AD intervention.

In conclusion, we have designed two novel bis-MEP derivatives ZLA and ZLB, and preliminarily evaluated their chemical properties and potencies of prevention of Aβ aggregation. They show potent AChE inhibition activity and are able to retard AChE-induced Aβ fibrillogenesis,

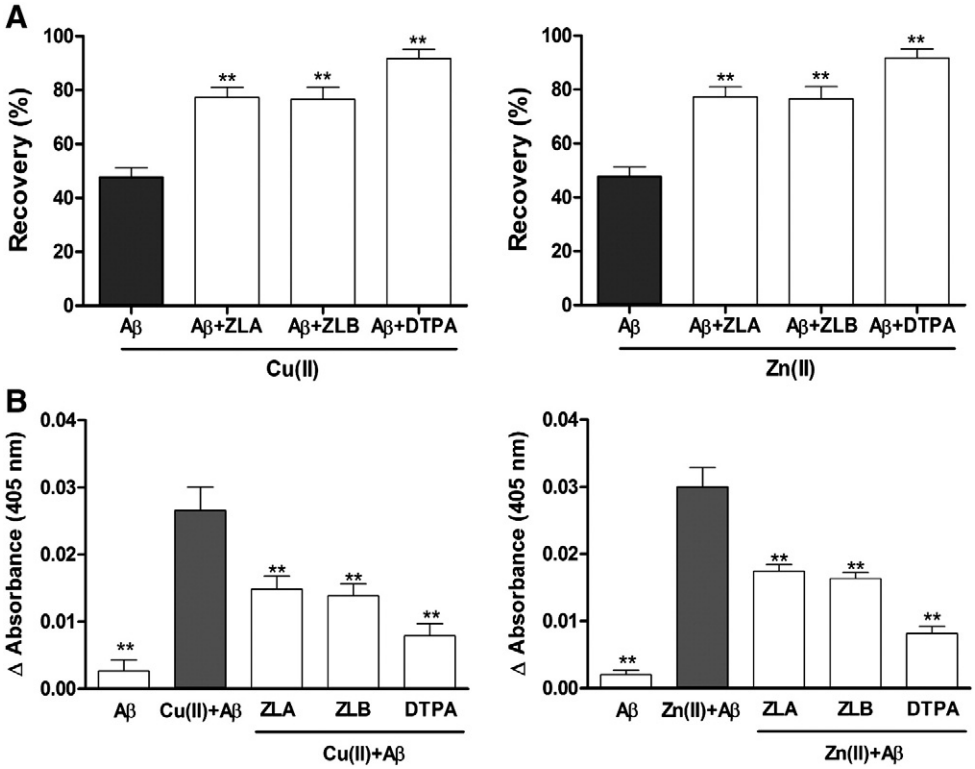

Fig. 7. Inhibition of ZLA or ZLB on Cu(II) or Zn(II)-induced Aβ1–40 aggregation. A) Recovery of Aβ1–40 following incubation with Cu(II) or Zn(II) and centrifugation (13,000×g, 15 min), expressed as percentage of the control (Aβ1–40 alone). B) Turbidometric analysis of Cu(II) or Zn(II)-induced Aβ Aggregation. Aβ1–40 (10 μM) were incubated with Cu(II) or Zn(II) (20 μM) for 15 min (A) or 30 min (B) at 37 °C, in the absence or presence of test compounds (100 μM) in 20 mM Hepes buffer, 150 mM NaCl (pH 6.6). The data indicate the mean ± SEM of three independent experiments. DTPA, diethylenetriamine pentaacetic acid, was used as a positive reference. $^{**}P<0.01$ versus Cu(II) + Aβ or Zn(II) + Aβ.

with IC_{50} values compatible to those for AChE inhibition. Concurrently, they also show additional Cu(II) or Zn(II)-complexing properties, and markedly prevent Aβ aggregation triggered by these metal ions. These results suggest that ZLA and ZLB may act as dual binding site AChEIs with additional metal ions-chelating potency. Therefore, they may represent promising lead candidates for design of multi-target-directed drugs for AD therapy.

Conflict of interest statement

The authors have no conflicts of interest.

Acknowledgments

We gratefully acknowledge financial support from the National Natural Science Foundation of China (Grant Nos. 30973538, 30973509 and 30801393), the National Innovative Drug Development Project (No. 2009ZX09103), the Shanghai Municipal Science and Technology Commission (No. 10431902700), and "Chen Guang" project supported by Shanghai Municipal Education Commission and Shanghai Education Development Foundation (No. 10CG03).

References

Atwood, C.S., Moir, R.D., Huang, X., Scarpa, R.C., Bacarra, N.M., Romano, D.M., Hartshorn, M.A., Tanzi, R.E., Bush, A.I., 1998. Dramatic aggregation of Alzheimer Aβ by Cu(II) is induced by conditions representing physiological acidosis. J. Biol. Chem. 273, 12817–12826.

Bajda, M., Guzior, N., Ignasik, M., Malawska, B., 2011. Multi-target-directed ligands in Alzheimer's disease treatment. Curr. Med. Chem. 18, 4949–4975.

Bartolini, M., Bertucci, C., Cavrini, V., Andrisano, V., 2003. β-Amyloid aggregation induced by human acetylcholinesterase: inhibition studies. Biochem. Pharmacol. 65, 407–416.

Baum, L., Ng, A., 2004. Curcumin interaction with copper and iron suggests one possible mechanism of action in Alzheimer's disease animal models. J. Alzheimers Dis. 6, 367–377.

Bolognesi, M.L., Cavalli, A., Valgimigli, L., Bartolini, M., Rosini, M., Andrisano, V., Recanatini, M., Melchiorre, C., 2007. Multi-target-directed drug design strategy: from a dual binding site acetylcholinesterase inhibitor to a trifunctional compound against Alzheimer's disease. J. Med. Chem. 50, 6446–6449.

Cater, M.A., McInnes, K.T., Li, Q.X., Volitakis, I., La Fontaine, S., Mercer, J.F., Bush, A.I., 2008. Intracellular copper deficiency increases amyloid-β secretion by diverse mechanisms. Biochem. J. 412, 141–152.

Duce, J.A., Bush, A.I., 2010. Biological metals and Alzheimer's disease: implications for therapeutics and diagnostics. Prog. Neurobiol. 92, 1–18.

Ennis, C., Haroun, F., Lattimer, N., 1986. Can the effects of meptazinol on the guinea-pig isolated ileum be explained by inhibition of acetylcholinesterase? J. Pharm. Pharmacol. 38, 24–27.

Faux, N.G., Ritchie, C.W., Gunn, A., Rembach, A., Tsatsanis, A., Bedo, J., Harrison, J., Lannfelt, L., Blennow, K., Zetterberg, H., Ingelsson, M., Masters, C.L., Tanzi, R.E., Cummings, J.L., Herd, C.M., Bush, A.I., 2010. PBT2 rapidly improves cognition in Alzheimer's disease: additional phase II analyses. J. Alzheimers Dis. 20, 509–516.

Fernández-Bachiller, M.I., Pérez, C., González-Muñoz, G.C., Conde, S., López, M.G., Villarroya, M., García, A.G., Rodríguez-Franco, M.I., 2010. Novel tacrine-8-hydroxyquinoline hybrids as multifunctional agents for the treatment of Alzheimer's disease, with neuroprotective, cholinergic, antioxidant, and copper-complexing properties. J. Med. Chem. 53, 4927–4937.

Furukawa-Hibi, Y., Alkam, T., Nitta, A., Matsuyama, A., Mizoguchi, H., Suzuki, K., Moussaoui, S., Yu, Q.S., Greig, N.H., Nagai, T., Yamada, K., 2011. Butyrylcholinesterase inhibitors ameliorate cognitive dysfunction induced by amyloid-β peptide in mice. Behav. Brain Res. 225, 222–229.

Greig, N.H., Utsuki, T., Ingram, D.K., Wang, Y., Pepeu, G., Scali, C., Yu, Q.S., Mamczarz, J., Holloway, H.W., Giordano, T., Chen, D., Furukawa, K., Sambamurti, K., Brossi, A., Lahiri, D.K., 2005. Selective butyrylcholinesterase inhibition elevates brain acetylcholine, augments learning and lowers Alzheimer β-amyloid peptide in rodent. Proc. Natl. Acad. Sci. U. S. A. 102, 17213–17218.

Guay, D.R., 2004. Drugs that target metal β-amyloid interactions can effect Alzheimer's disease. Commentary: metal-protein attenuation with iodochlorohydroxyquine (clioquinol) targeting β-amyloid deposition and toxicity in Alzheimer disease: a pilot phase 2 clinical trial. Consult. Pharm. 19, 637–638.

Hung, Y.H., Bush, A.I., Cherny, R.A., 2010. Copper in the brain and Alzheimer's disease. J. Biol. Inorg. Chem. 15, 61–76.

Inada, Y., Ozutsumi, K., Funahashi, S., Soyama, S., Kawashima, T., Tanakal, M., 1993. Structure of copper(II) ethylenediamine complexes in aqueous and neat ethylenediamine solutions and solvent-exchange kinetics of the copper(II) ion in ethylenediamine as studied by EXAFS and NMR methods. Inorg. Chem. 32, 3010–3014.

Inestrosa, N.C., Dinamarca, M.C., Alvarez, A., 2008. Amyloid–cholinesterase interactions. Implications for Alzheimer's disease. FEBS J. 275, 625–632.

Johnson, G., Moore, S.W., 2006. The peripheral anionic site of acetylcholinesterase: structure, functions and potential role in rational drug design. Curr. Pharm. Des. 12, 217–225.

Li, J., Huang, H., Miezan-Ezoulin, J.M., Gao, X.L., Massicot, F., Dong, C.Z., Heymans, F., Chen, H.Z., 2007. Pharmacological profile of PMS777, a new AChE inhibitor with PAF antagonistic activity. Int. J. Neuropsychopharmacol. 10, 21–29.

Mancuso, M., Orsucci, D., LoGerfo, A., Calsolaro, V., Siciliano, G., 2010. Clinical features and pathogenesis of Alzheimer's disease: involvement of mitochondria and mitochondrial DNA. Adv. Exp. Med. Biol. 685, 34–44.

Minarini, A., Milelli, A., Tumiatti, V., Rosini, M., Simoni, E., Bolognesi, M.L., Andrisano, V., Bartolini, M., Motori, E., Angeloni, C., Hrelia, S., 2012. Cystamine–tacrine dimer: a new multi-target-directed ligand as potential therapeutic agent for Alzheimer's disease treatment. Neuropharmacology 62, 997–1003.

Paz, A., Xie, Q., Greenblatt, H.M., Fu, W., Tang, Y., Sliman, I., Qiu, Z., Sussman, J.L., 2009. The crystal structure of a complex of acetylcholinesterase with a bis-(−)-nor-meptazinol derivative reveals disruption of the catalytic triad. J. Med. Chem. 52, 2543–2549.

Quinn, J.F., Harris, C.J., 2010. A copper-lowering strategy attenuates amyloid pathology in a transgenic mouse model of Alzheimer's disease. J. Alzheimers Dis. 21, 903–914.

Quinn, J.F., Crane, S., Harris, C., Wadsworth, T.L., 2009. Copper in Alzheimer's disease: too much or too little? Expert Rev. Neurother. 9, 631–637.

Raman, B., Ban, T., Yamaguchi, K., Sakai, M., Kawai, T., Naiki, H., Goto, Y., 2005. Metal ion-dependent effects of clioquinol on the fibril growth of an amyloid β peptide. J. Biol. Chem. 280, 16157–16162.

Schliebs, R., Arendt, T., 2011. The cholinergic system in aging and neuronal degeneration. Behav. Brain Res. 221, 555–563.

Venneri, A., McGeown, W.J., Shanks, M.F., 2005. Empirical evidence of neuroprotection by dual cholinesterase inhibition in Alzheimer's disease. Neuroreport 16, 107–110.

Xie, Q., Wang, H., Xia, Z., Lu, M., Zhang, W., Wang, X., Fu, W., Tang, Y., Sheng, W., Li, W., Zhou, W., Zhu, X., Qiu, Z., Chen, H., 2008. Bis-(−)-nor-meptazinols as novel nanomolar cholinesterase inhibitors with high inhibitory potency on amyloid-β aggregation. J. Med. Chem. 51, 2027–2036.

Yates, C.M., Butterworth, J., Tennant, M.C., Gordon, A., 1990. Enzyme activities in relation to pH and lactate in postmortem brain in Alzheimer-type and other dementias. J. Neurochem. 55, 1624–1630.